Molecular Crystals and Liquid Crystals Science and Technology. Section A. Molecular Crystals and Liquid Crystals

Publication details, including instructions for authors and subscription information:
http://www.tandfonline.com/loi/gmcl19

The Linear and Nonlinear Optical Properties of Nanometer-sized In_2O_3 Organosol

Wu Xiaochuw [a], Wang Rongyao [a], Zou Bingsuo [a], Xu Jiren [a], Yu Baolong [b], Tang Guoqing [b], Zhang Guilan [b] & Chen Wenju [b]

[a] The Institute of Physics, Chinese Academy of Science, Beijing, 100080

[b] The Institute of Modem Optics, Nankai University, Tianjin, 300071

Version of record first published: 04 Oct 2006

To cite this article: Wu Xiaochuw, Wang Rongyao, Zou Bingsuo, Xu Jiren, Yu Baolong, Tang Guoqing, Zhang Guilan & Chen Wenju (1997): The Linear and Nonlinear Optical Properties of Nanometer-sized In_2O_3 Organosol, Molecular Crystals and Liquid Crystals Science and Technology. Section A. Molecular Crystals and Liquid Crystals, 300:1, 283-293

To link to this article: http://dx.doi.org/10.1080/10587259708042354

Mol. Cryst. Liq. Cryst., 1997, Vol. 300, pp. 283–293
Reprints available directly from the publisher
Photocopying permitted by license only

The Linear and Nonlinear Optical Properties of Nanometer-sized In_2O_3 Organosol

WU XIAOCHUN[a], WANG RONGYAO[a], ZOU BINGSUO[a], XU JIREN[a], YU BAOLONG,[b] TANG GUOQING[b], ZHANG GUILAN[b] and CHEN WENJU[b]

[a]*The Institute of Physics, Chinese Academy of Science, Beijing, 100080;*
[b]*The Institute of Modern Optics, Nankai University, Tianjin, 300071*

(Received 30 November 1996; In final form 4 January 1996)

The linear and nonlinear optical properties of nanometer-sized In_2O_3 organosol were investigated by using TEM, ESR, UV-visible absorption spectrum, photoluminescence spectra and Z-scan technique. It was found that the prepared In_2O_3 organosol showed a series of new optical properties, which can be explained by its special structure. These new optical properties made its application in information optics enlarged.

Keywords: Optical properties; nanometer-sized In_2O_3; structure

1. INTRODUCTION

R. K. Jain and R. C. Lind measured large third-order optical nonlinear susceptibility and ultrafast carrier combination time in the semiconductor microcrystallite doped filter glass in 1985 [1]. From then on, semiconductor nanoparticles as a new kind of optical material have attracted great attention. Up to now, the various properties of nanometersized semiconductor materials have been studied and made great progress. The various effects which influence the properties of nanometer-sized materials, such as quantum size effect [2], surface effect [3], and local field effect [4], have been investigated. In one word, the studies of nanometer-sized semiconductor materials have entered a prosperous period [5].

In_2O_3 in bulk is being extensively utilized. It also has relatively large nonresonant third-order nonlinear optical susceptibility among inorganic oxides [6]. In order to study its optical properties under nanometer-size range, nanometer-sized In_2O_3 organosol was synthesized and characterized through a series of spectroscopic techniques.

2. EXPERIMENTS

2.1. Synthesis of In_2O_3 Nanoparticles

Nanometer-sized In_2O_3 organosol was prepared through microemulsion method. 10 ml of newly-made $InCL_3$ aqueous solution (0.1 M) was added to 100 ml of toluene containing 1×10^{-3} mol of stearic acid. The resulting mixture was stirred to form microemulsion, then 20 ml of 0.1 M NaOH aqueous solution was added by means of a pipet to the microemulsion to produce hydroxide under strong stirring. After the reaction completed, the reaction product was extracted into the organic phase because its surface was capped with a layer of stearic acid, then let the reaction system stand still to separate the organic phase from the water phase. The water phase was discarded and the organic phase was refluxed 0.5 hr, then cooled to room temperature. The little amount of water on the bottom of the flask was discarded and the organic phase was washed with distilled water for several times to further purify the reaction product. After the purification, the organic phase was distilled to remove the remnant water. Finally nanometer-sized In_2O_3 organosol with concentration of 5×10^{-3} M was synthesized.

2.2. Measurement Methods

The size of nanoparticle organosol was measured through Philips EM-400 transmission electron microscopy (TEM). The average particle diameter was 6 nm as shown in Figure 1. Absorption and photoluminescence spectra were measured by Shimadzu UV-240 spectrophotometer and a RF-540 fluorimeter, respectively. ESR measurement was performed on Bruker 200D-SRC spectrometer. The magnetic field was calibrated with Mn^{2+} as a standard. Continuous wave (cw) laser Z-scan measurement was carried with a cw Ar^+ laser as light sources. Pulse laser Z-scan measurement was carried out with 18-ns, 1.06 μm pulse from a Q-switched Nd:YGA laser, operating at a repetition rate 1Hz, as the excitation light source. In which nonlinear-optical signals were compared with that obtained from a reference sample of CS_2

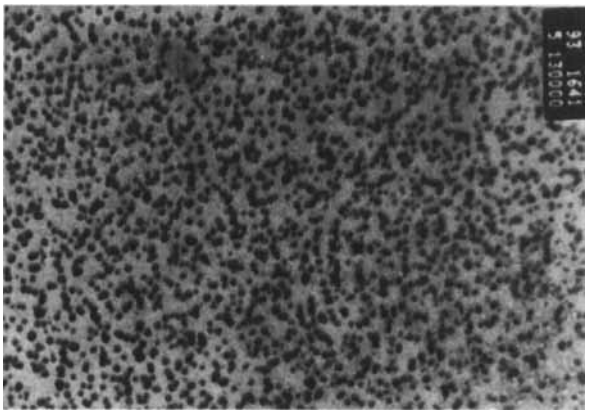

FIGURE 1 The TEM bright field image of nanometer-sized In_2O_3 organosol.

under the same experimental conditions. All experiments were performed at room temperature.

3. RESULTS AND DISCUSSION

3.1. Absorption Spectrum

The absorption of stearic acid and toluene appears at wavelength shorter than 300 nm and can be neglected. Figure 2 represents the absorption spectrum of the sample. It could be seen that when wavelength is longer than 350 nm, (band gap in bulk), the sample still has strong absorption. The absorption coefficient of amorphous semiconductor can be written as [7]:

$$\alpha\hbar\omega = A(\hbar\omega - E_g)^2 \tag{1}$$

α, $\hbar\omega$, E_g are absorption coefficient; photo energy, apparent optical band-gap respectively. A is a constant. From the formula (1) it could be seen that $(\alpha\hbar\omega)^{1/2}$ has a linear relation with $\hbar\omega$, the slope of straight line gives E_g of materials. The E_g of sample is 2.3 eV, which red-shifts 1.2 eV compared with that of bulk In_2O_3 [8]. This is contrary to the quantum size effect which leads to the blue-shift of E_g. with the decrease of particle size and has been observed in many nanometer-sized semiconductor materials [9]. Since the particle radius (30A) of the sample is larger than the exciton Bohr radius of

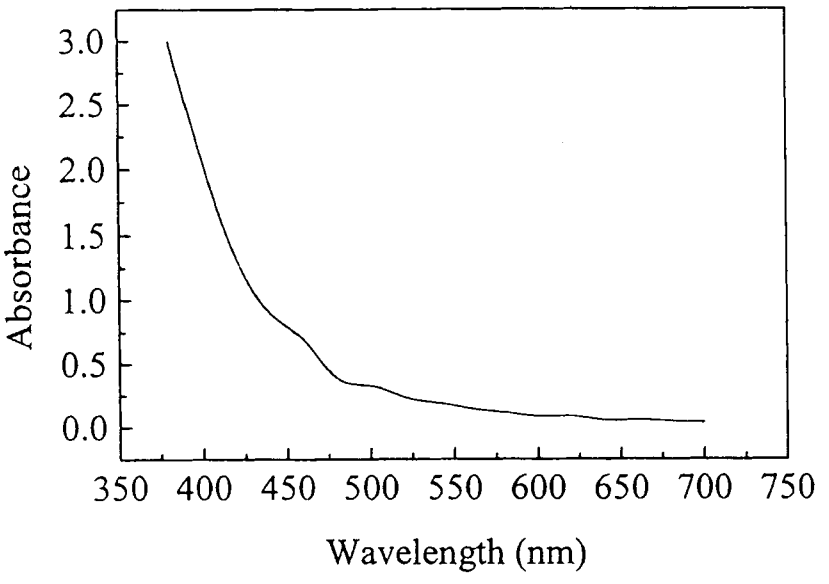

FIGURE 2 The absorption spectrum of nanometer-sized In_2O_3 organosol.

bulk In_2O_3, 10A [10], the sample belongs to weak confinement and the blue-shift of absorption band-gap, due to the quantum size effect, is very small and can be neglected. On the other hand, from the analysis of sample preparation process the amount of In^{3+} used in reaction is stoichiometrically larger than that of OH in order to ensure the prepared nanoparticles to have positive charges, which attract anionic surfactants to adsorb to the nanoparticles surface to form stable nanoparticles as shown in preparation process. Therefore, there are lots of oxygen vacancies due to non-stoichiometic ratios of reactants, which mainly locate in the interface of nanoparticles and have strong interaction with the interfacial capping surfactants. This interaction stabilized the interfacial oxygen vacancies and make them form a series of metastable energy levels within the forbidden band. This leads to the red-shift of optical band-gap of the prepared sample in absorption spectrum.

The existence of oxygen vacancies was further justified by the ESR spectrum as shown in Figure 3. In_2O_3 in bulk is an antimagnetic material, whereas the prepared In_2O_3 organosol shows an obvious ESR signal which stably exists at room temperature. The g factor of the sample is 2.001, which is similar to the g-factor of a F center formed by electron capture by an O^{2-} vacancy [11]. This indicates that there certainly exist interfacial oxygen

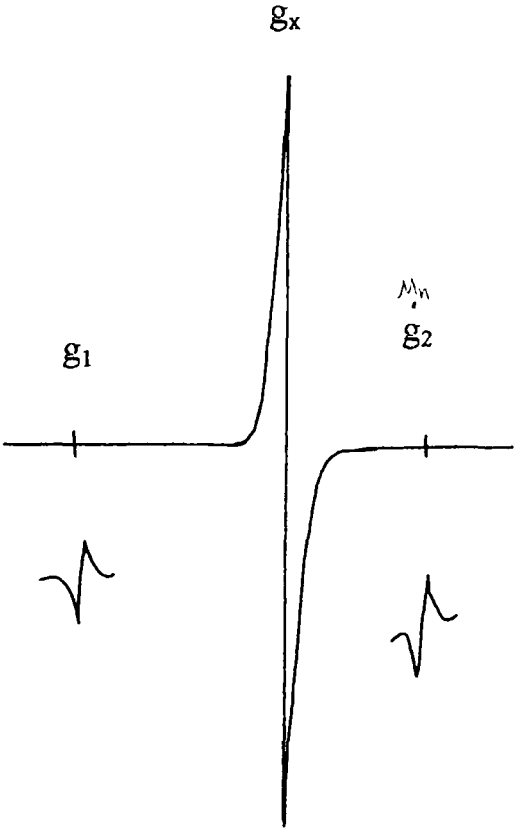

FIGURE 3 The ESR spectrum of nanometer-sized In_2O_3 organosol at room temperature a: microwave frequency: 9.3 GHz; b: microwave power: 1mW; c: modulation frequency: 100 KHz; d: modulation amplitude: 2 Gauss.

vacancies in the prepared sample, which trap electrons to form paramagnetic centers to provide the observed ESR signal.

3.2. Excitation and Photoluminescence Spectra

In_2O_3 in bulk has no luminescence at room temperature [10], while the prepared sample shows obvious photoluminescence at room temperature as shown in Figure 4b,c. Figure 4a is the excitation spectrum of the sample with emissions wavelength of $\lambda_{em} = 520$ nm, which exhibits a wide excitation band with wavelength range from 350 to 500 nm coinciding with the absorption band of oxygen vacancies. This implies that the absorption of oxygen vacancies contributes to the observed emission. The structures of

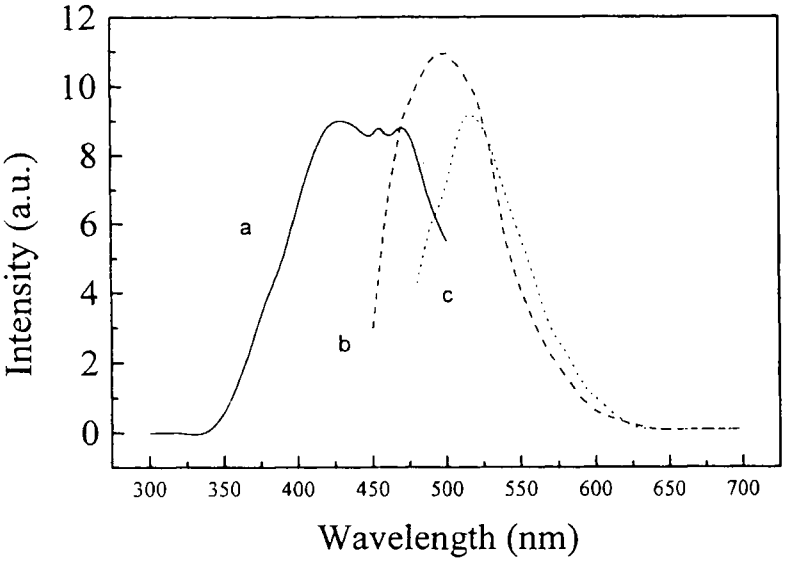

FIGURE 4 The excitation and photoluminescence spectra of nanometer-sized In_2O_3 organosol. a: The excitation spectrum of $\lambda_{em} = 520$ nm, b: The fluorescence spectrum of $\lambda_{ex} = 430$ nm, $\lambda_{em,max} = 495$ nm; c: The fluorescence spectrum of $\lambda_{ex} = 470$ nm, $\lambda_{em,max} = 518$ nm.

excitation spectrum and photoluminescence spectra reflect the structural and environmental complexities of those oxygen vacancies. These energy levels of oxygen vacancies are a series of metastable energy levels which have relatively long lifetimes and the optical transitions are dipole-allowed.

From absorption and luminescence spectra, it can be concluded that due to the existence of this special interfacial oxygen vacancies stabilized by the capping surfactants, these oxygen vacancies form a series of metastable levels within the prohibited band of In_2O_3. The formation of these metastable leads to the red-shift of absorption band-edge and photoluminescence at room temperature due to their relatively long lifetimes.

3.3. Z-Scan Study

Z-scan technique is a simple, sensitive, single-beam method that uses the principle of spatial beam distortion to measure the sign and magnitude of refractive nonlinearities (n_2) of optical materials. The details of the estimation procedures and theoretical background are well documented in the literatures [12, 13].

The third-order optical nonlinear susceptibilities of stearic acid and toluene are smaller than 10^{-12} esu and can be neglected. The Z-scan curves of the sample excited with pulse laser is shown in Figure 5. The Z-scan curve of sample, with closed-aperture arrangement, as shown in Figure 5a indicates that the sample belongs to defocusing materials and exists multiphoton absorption as discussed above. Figure 5b further justifies the existence of multiphoton absorption with open-aperture arrangement. The ratio of two curves gives pure refractive nonlinearity. Through calculation, the pure nonlinear refractive coefficient n_2 is about -3.4×10^{-10} esu, which is two-order magnitude larger than that of bulk In_2O_3, 1.7×10^{-12} esu and is opposite in sign of nonlinearity. The excitation of sample at 1.06 μm belongs to nonresonant excitation because sample has no absorption at this wavelength. Therefore, the nonlinearities of thermalized refractive change and exciton effect due to linear absorption can be neglected. The origin of optical nonlinearity is mainly electronic refractive effect. Cotter *et al.* [14] had reported an investigation of the behaviors of $\chi^{(3)}$ in the transparency region for semiconductor microcrystallites using Z-scan method. They found that the electronic refractive nonlinearity of a series of semiconductor microcrystallites embedded in a glass matrix with particle radius range from

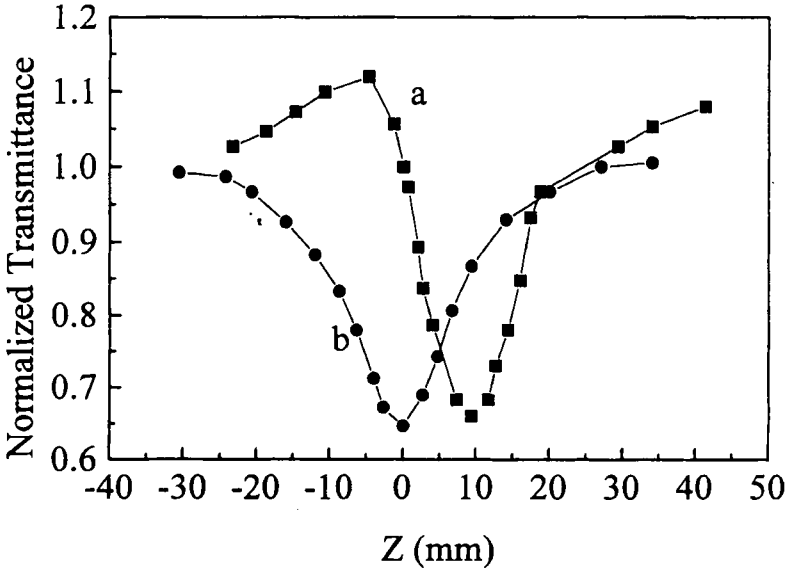

FIGURE 5 Z-scan normalized transmittance of nanometer-sized In_2O_3 organosol excited by Q-switched nd: YAG laser with a peak irradiance I_0 of 0.21 GW/cm^2 a: closed-aperture ($S = 0.34$); b: open-aperture ($S = 1$).

3.5 nm to 6.5 nm (1–2.5 times the electron Bohr radius) are consistently negative in sign for frequencies below the absorption edge, indicating the dominant role of the optical stark effect, which is different from that of bulk semiconductors. They further pointed out that even in weak confinement region, the quantum size confinement has a profound influecne of $\mathrm{Re}\chi^{(3)}$ in the transparency region only if the excitation of sample is on or near resonance for 2PA(two-photon absorption). The quantum confinement would be expected to influence this process strongly and correspondingly affect the optical stark effect. In our sample (particle radius 3 times exciton Bohr radius), the $\mathrm{Re}\chi^{(3)}$ (n_2) is also negative and the excitation of the prepared sample is on 2PA resonance. Therefore the increase of $\mathrm{Re}\chi^{(3)}$ of our sample partly come from the contribution of this process, whereas in bulk In_2O_3 the optical stark effect at this wavelength can be neglected due to its excitation far-away from the 2PA resonance ($2\hbar\omega \ll E_g$). Our experimental results agree with those of Cotter *et al.* Undoubtedly, the contribution of the interfacial oxygen vacancies is most important. On the one hand, they lead to the red-shift of absorption band-edge and make the excitation of sample at this wavelength satisfy the condition of 2PA resonance enhancement of optical stark effect; on the other hand, these oxygen vacancies with negative charges will produce a strong electric field which will further enhance optical stark effect and finally increase $\mathrm{Re}\chi^{(3)}$ of the sample. Therefore Both interfacial oxygen vacancies and quantum size effect contribute to the increase of $\mathrm{Re}\chi^{(3)}$ in our prepared sample. It can be obtained from the analysis of absorption spectrum that the band-gap of sample located at the wavelength of 540 nm, which is just longer than that of double frequency of 1.06 μm laser and satisfies the condition of two-photon absorption, $E_g < \hbar\omega < 2E_g$. The two-photon absorption coefficient β ($\mathrm{Im}\chi^{(3)}$) which was obtained through open-aperture arrangement, is 0.15 cm/GW.

One of the applications of nonlinear refractive index is in the role of all-optical switching. The ratio $n_2/\beta\lambda$, which is a vital parameter for device, is 310 and quite large. Therefore our prepared sample is a quite good material for all-optical switching device.

The Z-scan curves of sample excited with a cw Ar^+ laser as shown in Figure 6 indicated that the refractive nonlinearity also belongs to defocusing nonlinearity, while the absorptive nonlinearity belongs to saturation absorption. The n_2 of sample at 514.5 nm is -5.8×10^{-5} esu, and the saturation absorption light intensity Isat is equal to 200 mW/cm^2, which is much low and indicates its application in optical limiting at visible light range. The excitation of sample with a cw Ar^+ laser at 514.5 nm belongs to resonant excitation because excitation wavelength is shorter than band-edge

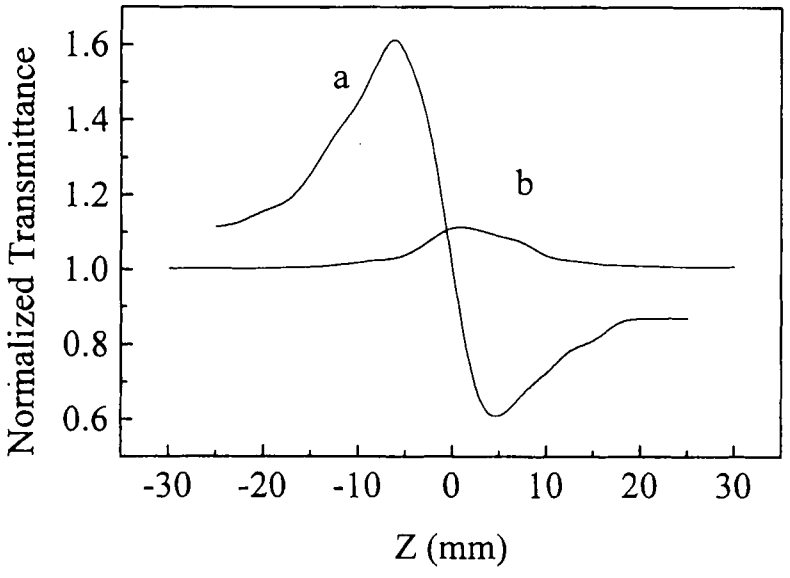

FIGURE 6 Z-scan normalized transmittance of nanometer-sized In_2O_3 organosol excited with a cw Ar^+laser. a: closed-aperture ($S = 0.34$) with total irradiance I_0 of 0.1 MW/cm^2; b: open-aperture ($S = 1$) with total irradiance I_0 of 0.83 MW/cm^2.

wavelength. From the analysis of linear spectra, on the one hand, it becomes clear that the excitation of sample at $\lambda = 514.5$ nm gives rise to from oxygen vacancies at the interface of nanoparticels, which shows strong electron-lattice interaction due to its strong interaction with capping surfactants and disorder of interfacial structure [15,16]. The strong electron-lattice interaction indicates that the system has high non-irradiative efficiency, which can leads to large thermalized refractive nonlinearity at strong laser irradiation. Therefore the large n_2 of sample at 514.5 nm comes from thermalized refractive change. On the other hand, those oxygen vacancies exist in the form of metastable states, which have relatively long life times. The excitation of those long-lifetime metastable states at strong laser irradiation can lead to the nonlinear saturation absorption. The low saturation intensity of sample is due to the long lifetime of those oxygen vacancies.

4. CONCLUSIONS

From above experiments and discussion, it could be concluded that the structure of the prepared nanometer-sized In_2O_3 nanoparticles consists of

the inner In_2O_3 microcrystallite core covered with a shell of interfacial oxygen vacancies stabilized by surfactants, similar to that of porous silicon [17]. This special oxygen vacancy structures make nanometer-sized In_2O_3 nanoparticles exhibit a series of new linear and nonlinear optical properties which can be summarized as follows:

(1) The nanometer-sized In_2O_3 organosol shows red-shift of absorption band-edge due to the formation of metastable energy levels of oxygen vacancies within the prohibited band.
(2) These metastable energy levels emit obvious fluorescence at room temperature due to their relatively long lifetimes.
(3) The existence of oxygen vacancies is further justified through ESR spectrum.
(4) From the pulse laser Z-scan study at the wavelength of 1.06 μm, the n_2 of the sample is -3.4×10^{-10} esu mainly coming from the optical stark effect, larger than that of the bulk. Due to the red-shift of band-gap, the two-photon absorption is also observed at this wavelength and β is 0.5 cm/GW.
(5) From the cw laser Z-scan study at the wavelength of 514.5 nm, the n_2 of the sample is -5.8×10^{-5} esu coming from the contribution of thermalized refraction. Due to the excitation of metastable energy levels of long life-time at this wavelength, obvious saturation absorption phenomenon is observed and Isat is 6.55 W/cm^2.

These new optical properties can be reasonably explained by its special oxygen vacancy structures under nanometer-sized range. These new optical properties also enlarge the applications of In_2O_3 in nonlinear optics, such as optical switching and optical limiting.

Acknowledgement

The authors acknowledge the National Natural Science Foundation of China for financial support.

References

[1] R. K. Jain and R. C. Lind, *J. Opt. Soc. Am.*, **73**, 647 (1983).
[2] A. Henglein, *Chem. Rev.*, **89**, 1861 (1989).
[3] Y. Wang and N. Herron, *J. Phys. Chem.*, **91**, 5005 (1987).
[4] Y. Wang and N. Herron, *J. Phys. Chem.*, **95**, 525 (1991).
[5] A. D. Yoffe, *Adv. Phys.*, **42**, 173 (1993).
[6] W. J. Nie, *Adv. Mater.*, **5**, 520 (1993).
[7] G. Mill, Z. G. Li and D. Meisel, *J. Phys. Chem.*, **92**, 822 (1988).
[8] Y. Ohhata, F. Shinoki and S. Yoshida, *Thin Solid Films*, **59**, 255 (1979).

[9] L. E. Brus, *Appl. Phys.*, **A 53**, 465 (1991).
[10] Z. M. Jarzebski, *Phys. Stat. Sol.*, (a) **71**, 13 (1982).
[11] T. Z. Jin, D. Zh Wang, S. H. Jin, *Chinese Phys. Lett.*, **9**, 549 (1992).
[12] S. B. Mansor, A. A. Said and W. E. VanStryland, *Opt. Lett.*, **14**, 955 (1989).
[13] S. B. Mansor, A. A. Said and W. E. VanStryland, *IEEE J. Quantum Electron.*, **26**, 760 (1990).
[14] D. Cotter, M. G. Burt and R. J. Manning, *Phys. Rev. Lett.*, **68**, 1200 (1992).
[15] Yu. M. Galperin, V. G. Karpov and V. I. Kozub, *Adv. Phys.*, **38**, 669 (1989).
[16] St. Pnevmatikos, O. Yanovitskii, Th. Friggis and E. N. Econornou, *Phys. Rev. Lett.*, **68**, 2370 (1992).
[17] Y. Kanemitsu, *Phys. Reports*, **263**, 1 (1995).